THE JOURNAL OF BIOLOGICAL CHEMISTRY
Vol. 277, No. 45, Issue of November 8, pp. 43262–43270, 2002

Printed in U.S.A.

Reversible Unfolding of FtsZ Cell Division Proteins from Archaea and Bacteria

COMPARISON WITH EUKARYOTIC TUBULIN FOLDING AND ASSEMBLY*

Received for publication, July 8, 2002, and in revised form, August 25, 2002
Published, JBC Papers in Press, September 4, 2002, DOI 10.1074/jbc.M206723200

José Manuel Andreu‡§, María Angela Oliva‡, and Octavio Monasterio¶

From the ‡Centro de Investigaciones Biológicas, Consejo Superior de Investigaciones Científicas, Velázquez 144, 28006 Madrid, Spain and the ¶Departamento de Biología, Facultad de Ciencias, Universidad de Chile, Casilla 653, Santiago, Chile

The stability, refolding, and assembly properties of FtsZ cell division proteins from *Methanococcus jannaschii* and *Escherichia coli* have been investigated. Their guanidinium chloride unfolding has been studied by circular dichroism spectroscopy. FtsZ from *E. coli* and tubulin released the bound guanine nucleotide, coinciding with an initial unfolding stage at low denaturant concentrations, followed by unfolding of the apoprotein. FtsZ from *M. jannaschii* released its nucleotide without any detectable secondary structural change. It unfolded in an apparently two-state transition at larger denaturant concentrations. Isolated FtsZ polypeptide chains were capable of spontaneous refolding and GTP-dependent assembly. The homologous eukaryotic tubulin monomers misfold in solution, but fold within the cytosolic chaperonin CCT. Analysis of the extensive tubulin loop insertions in the FtsZ/tubulin common core and of the intermolecular contacts in model microtubules and tubulin-CCT complexes shows a loop insertion present at every element of lateral protofilament contact and at every contact of tubulin with CCT (except at loop T7). The polymers formed by purified FtsZ have a distinct limited protofilament association in comparison with microtubules. We propose that the loop insertions of tubulin and its CCT-assisted folding coevolved with the lateral association interfaces responsible for extended two-dimensional polymerization into microtubule polymers.

The eukaryotic cytoskeletal proteins actin and tubulin probably have common ancestors with their respective prokaryotic homologs MreB (1) and FtsZ (2). MreB is a nucleotide-binding protein that is essential for bacterial rod shape (3), whereas the GTP-binding protein FtsZ is the key component of the prokaryotic cell division machinery (4). Archaeal FtsZ from *Methanococcus jannaschii* (2) and eukaryotic tubulin (5) share a common core of similarly folded N-terminal nucleotide-binding and middle structural domains. Their main differences include the tubulin C-terminal domain and several of the complex surface loops of tubulin; however, most of the seven nucleotide-binding loops are well conserved between FtsZ and tubulin, which constitute a distinct family of GTPases (6). No structure of a bacterial FtsZ has so far been reported. Tubulin $\alpha\beta$-dimers assemble into microtubules, long cylinders made of laterally associated protofilaments that form the mitotic spindle. Tubulin interacts with microtubule-associated proteins and with motor proteins mainly through its C-terminal domains. Docking the electron crystallographic structure of tubulin dimers (5, 7) into lower resolution electron density maps of microtubules has generated pseudo-atomic models of microtubules (8–10). On the other hand, FtsZ assembles at the future site of cell division, forming the so called Z-ring (11, 12), the structure of which has resisted observation. The Z-ring is stabilized by the binding of the C-terminal end of FtsZ to cell division proteins FtsA and ZipA; FtsA and ZipA recruit FtsK, which in turn interacts with the other septal proteins FtsQ, FtsL, FtsW, FtsI, and FtsN (4, 13). FtsZ monomers form *in vitro* polymers made of tubulin-like protofilaments with the characteristic 4-nm axial spacing (14, 15). Bacterial FtsZ expressed in mammalian cells does not co-assemble with microtubules, but can be induced to form other filaments (16). It is conceivable that the structural complexity of tubulin relative to FtsZ has evolved together with its assembly into microtubules.

Folding of many newly synthesized proteins in the cytosol is assisted by molecular chaperones (17). Actin and tubulin are the paradigm of eukaryotic proteins that require the cytoplasmic chaperonin CCT[1] (TriC) for their *in vivo* or *in vitro* folding (18–21). On the other hand, the ease of overproducing soluble FtsZ and MreB in bacteria suggests that these proteins may be able to fold spontaneously. In fact, FtsZ was not identified as an *in vivo* substrate of the bacterial chaperonin GroEL (although it is a two-$\alpha\beta$-domain protein), but the less abundant cell division inhibitor MinD was (22); and FtsZ did not bind to GroEL or CCT *in vitro* (23). However, HscA (a protein of the Hsp70 family) and DnaK have been implicated in FtsZ ring formation through a chaperone-like activity (24). Monomers of α- and β-tubulin bind to CCT in a quasi-native conformation in which the N-terminal, middle, and C-terminal domains are apparently opened up in the chaperonin cavity, and it has been proposed that the eukaryotic chaperonin coevolved with tubulin and actin (25, 26). Upon ATP binding, CCT undergoes a structural change that closes the tubulin monomer into its native GTP-binding conformation, followed by ATP hydrolysis by CCT and tubulin release (27).

In this work, we have investigated the stability, folding, and

* This work was supported in part by MCyT Grant BIO99-0859-C03-02/BIO2000-0748, the Programa de Grupos Estratégicos de la Comunidad de Madrid (to J. M. A.), an FPI predoctoral fellowship (to M. A. O.), and FONDECYT Grant 1010848 (to O. M.). The costs of publication of this article were defrayed in part by the payment of page charges. This article must therefore be hereby marked "*advertisement*" in accordance with 18 U.S.C. Section 1734 solely to indicate this fact.

§ To whom correspondence should be addressed. Tel.: 34-91-561-1800 (ext. 4380); Fax: 34-91-562-7518; E-mail: j.m.andreu@cib.csic.es.

[1] The abbreviations used are: CCT, chaperonia containing tailless polypeptide 1; GdmCl, guanidinium chloride; DTT, dithiothreitol; TCEP, tris(2-carboxyethyl)phosphine hydrochloride; Pipes, 1,4-piperazinediethanesulfonic acid; Mes, 4-morpholineethanesulfonic acid; GMPCPP, guanosine 5′-(α,β-methylenetriphosphate).

assembly ability of refolded FtsZ molecules in comparison with tubulin. For this purpose, we first studied the unfolding by guanidinium chloride (GdmCl) of FtsZ from the hyperthermophilic archaeon *M. jannaschii* and from the bacterium *Escherichia coli* by circular dichroism spectroscopy. The unfolding of *E. coli* FtsZ and of tubulin from calf brain was multistage, starting with nucleotide release. *M. jannaschii* FtsZ unfolded in a single stage at higher GdmCl concentrations at 25 °C; however, it released its nucleotide at lower denaturant concentrations. The unfolding of FtsZ by GdmCl was reversible, yielding refolded FtsZ capable of GTP-dependent assembly, whereas the denaturation transitions of tubulin could not be reversed. We further analyzed the structures and assemblies of FtsZ and tubulin, which suggest that the loop insertions of tubulin and its CCT-assisted folding coevolved with the lateral association interfaces responsible for two-dimensional polymerization into microtubules.

EXPERIMENTAL PROCEDURES

Proteins, Concentration Measurements, and Chemicals—M. jannaschii FtsZ with a C-terminal Gly-Ser-His_6 extension (M_r 39,891, 372 residues) (2) was overproduced in *E. coli* BL21(DE3) pLys and purified by HiTrap Ni^{2+} chelating affinity and Sephacryl S400 (Amersham Biosciences) size-exclusion chromatography. It typically contained ~0.8 nucleotide bound, of which 80% was GDP and 20% was GTP; and it was stored concentrated (10–30 mg ml^{-1}) at −70 °C (28). Its guanine nucleotide content was spectrophotometrically determined after extraction with cold 0.5 N $HClO_4$ employing an extinction coefficient of 12,400 M^{-1} cm^{-1} at 254 nm (29). The concentration of *M. jannaschii* FtsZ was determined from its absorption spectrum in 6 M GdmCl, after subtraction of the absorbance due to the guanine nucleotide (ϵ_{254} = 13,620 M^{-1} cm^{-1} and ϵ_{280} = 8100 M^{-1} cm^{-1} in 6 M GdmCl) (28), employing apoprotein extinction coefficients of ϵ_{280} = 6970 M^{-1} cm^{-1} and ϵ_{254} = 4275 M^{-1} cm^{-1} (calculated for 1 Trp, 1 Tyr, and 8 Phe residues) (30, 31). The approximate extinction coefficients determined for native *M. jannaschii* FtsZ are 11,600 M^{-1} cm^{-1} at 254 and 280 nm when containing 0.8 mol of nucleotide after dilution in neutral buffer and 13,000 M^{-1} cm^{-1} at 280 nm and 14,200^{-1} cm^{-1} at 254 nm when containing 1.0 mol of nucleotide typically after equilibration of the native protein in GDP- or GTP-containing buffer. *M. jannaschii* FtsZ without the unnatural Gly-Ser-His_6 extension was constructed from the same plasmid, pHis17-mjFtsZ-H_6 (2), and purified by ammonium sulfate precipitation and ion-exchange and hydrophobic chromatography.[2]

E. coli FtsZ (M_r 40,324, 383 residues) was overproduced in *E. coli* BL21(DE3) and purified by two cycles of Ca^{2+}-induced precipitation, followed by Mono Q anion-exchange chromatography (32). It typically contained 1.0 GDP bound per FtsZ and was stored concentrated (20–50 mg ml^{-1}) at −70 °C. Its concentration was spectrophotometrically determined in 6 M GdmCl, after subtraction of the nucleotide absorption (as described above), employing extinction coefficients of ϵ_{280} = 3840 M^{-1} cm^{-1} and ϵ_{254} = 2750 M^{-1} cm^{-1} (note that *E. coli* FtsZ has no Trp residues and 3 Tyr and 13 Phe residues).

Bovine brain tubulin $\alpha\beta$-dimers were purified by ammonium sulfate precipitation, batch DEAE-Sephadex anion-exchange chromatography, and Mg^{2+}-induced precipitation (33–35) and stored concentrated (~100 mg ml^{-1}) under liquid nitrogen. Tubulin $\alpha\beta$-dimers have 896 residues and a molecular weight of 99,929, calculated for the major tubulin isotypes from pig brain, not taking into account other isotypes and post-translational modifications (for review, see Ref. 36). Tubulin contained 1.6–2.0 mol of bound GTP. Tubulin dimer concentration was spectrophotometrically determined at 276 nm employing the previously measured extinction coefficients of 109,000 M^{-1} cm^{-1} in 6 M GdmCl (the value calculated as described above for 8 Trp and 35 Tyr residues and 1.8 ± 0.2 GTP is 109,000 ± 2000 M^{-1} cm^{-1}) and 116,000 M^{-1} cm^{-1} in neutral buffer after light scattering correction (34).

GdmCl and dithiothreitol (DTT) were from Calbiochem (Ultrol grade), and TCEP was from Interchim. Pipes, Hepes, Mes, and GDP were from Sigma. GTP (lithium salt) was from Roche Molecular Biochemicals. Other analytical grade chemicals were from Merck.

Circular Dichroism and Fluorescence Spectroscopy—CD spectra were acquired with Jasco 720 and 810 spectropolarimeters employing 1-mm cells in thermostatted cell holders (0.1- and 0.2-mm cells for spectra below 210 nm). The temperature was measured with a small thermocouple placed into the cells. Four scans of each sample or buffer (1-nm bandwidth and measurement interval, 20 nm min^{-1} scan speed, and 4-s time constant) were averaged, but not smoothed. Accurate CD measurements at fixed wavelengths were made from 5- to 10-min time recordings of each sample (10-s intervals and 16-s time constant). CD data (millidegrees) were reduced to mean residue ellipticity values (degrees cm^2 $dmol^{-1}$) with Jasco J700 and J800 software and plotted with SigmaPlot. Fluorescence measurements were made with a Fluorolog 3-221 instrument (Jobin Yvon-Spex, Longiumeau, France) employing 2-nm excitation and 5-nm emission bandwidths.

Protein Unfolding—Solutions of GdmCl were prepared gravimetrically, and their concentration was confirmed by refractometry (37). Concentrated protein stock solutions were diluted into 6 or 8 M GdmCl and 5 mM DTT solutions in buffer. Alternately, more concentrated FtsZ solutions in 6 M GdmCl were prepared by gravimetric addition of 1.009 mg of GdmCl/μl of protein stock. Proteins were held a minimum of 0.5 h in 6 M GdmCl at 25 °C before refolding. For protein refolding, the denaturant concentration was reduced by dialysis (4 °C, >16 h) or by dilution (50- or 100-fold) in buffer. Buffers were 20 mM Pipes-KOH and 5 mM DTT (pH 7.5) for FtsZ and 10 mM sodium phosphate and 5 mM DTT (pH 7.0) for tubulin.

Equilibrium GdmCl unfolding and refolding curves (37, 38) were determined by careful dilution of native and denatured proteins, respectively, into the corresponding GdmCl solutions in the same buffers with 5 mM DTT, followed by equilibration (in an Eppendorf Thermostat Plus) and CD measurements at 5 ± 1, 25 ± 1, and 42 ± 1 °C. At 25 °C, *M. jannaschii* FtsZ required a minimum of 36 h to reach equilibrium in the transition GdmCl range in both directions (but only a few minutes at 0 and 6 M GdmCl), whereas *E. coli* FtsZ required 2 h and tubulin required 1 h for equilibration at intermediate GdmCl concentrations. Measurements of GdmCl-induced unfolding of *M. jannaschii* FtsZ at 55 ± 1 and 70 ± 1 °C were made by directly taking CD time recordings until attainment of equilibrium (<100 min at 55 °C and <20 min at 70 °C) using cuvettes sealed with Teflon stoppers.

Nucleotide Release—Measurements of nucleotide release induced by GdmCl were made by protein depletion. The applicable conditions were designed simulating sedimentation with the program SIMCEN10 (kindly provided by Dr. Allen P. Minton, NIDDK, National Institutes of Health, Bethesda, MD) employing known molecular weights and sedimentation coefficients and were empirically confirmed in each case. Solutions of *M. jannaschii* FtsZ in 20 mM Pipes-KOH, 2 mM TCEP, and 0–4 M GdmCl (pH 7.5) were centrifuged in a Beckman TL120 rotor at 120,000 rpm for 4 h at 25 °C. The nucleotide released was spectrophotometrically measured in the upper half (0.5 ml) of each tube, which was carefully removed and found to be depleted of protein. Buffer blanks were employed, and the measurements were corrected by the small sedimentation of GDP in samples without protein. Solutions of *E. coli* FtsZ in 20 mM Pipes-KOH, 250 mM KCl, 2 mM TCEP, 10 μM GDP, and 0–1 M GdmCl (pH 7.5) were centrifuged for 3 h and measured as described above. Solutions of tubulin in 10 mM sodium phosphate, 2 mM DTT (which gave an acceptable interference in this case; 2 mM TCEP precipitated tubulin), 10 μM GTP, and 0–1 M GdmCl (pH 7.0) were centrifuged for 1 h and measured as described above.

FtsZ Assembly—Solutions of *M. jannaschii* FtsZ that had been dialyzed in the cold against 250–500 volumes of 20 mM Pipes-KOH, 2 mM DTT, and 10 μM nucleotide (pH 7.5) were brought to 50 mM Pipes-KOH, 2 mM DTT, 10 μM nucleotide, 50 mM KCl, and 1 mM EDTA (pH 6.5) (*M. jannaschii* FtsZ assembly buffer) at room temperature by addition of small volumes of concentrated Pipes-KOH (pH 6.5), KCl, EDTA, and HCl, and their concentrations were determined spectrophotometrically. Note that *M. jannaschii* FtsZ partially precipitated if directly transferred to cold *M. jannaschii* FtsZ assembly buffer due to the His_6 tag added for purification purposes.[2] *M. jannaschii* FtsZ was placed into a fluorometer cuvette thermostatted at 55 °C, and its 350 nm light scattering at a 90° angle was monitored with a Shimadzu RF540 spectrofluorometer operating in the ratio mode (2-nm excitation and emission band pass and ordinate scale of 1). *M. jannaschii* FtsZ assembly was initiated by addition of 6 mM $MgCl_2$ followed by 1 mM GTP to the cuvette. *E. coli* FtsZ in 6 M GdmCl or buffer was diluted 50- or 100-fold into cold 50 mM Mes-KOH, 50 mM KCl, 2 mM DTT, and 10 mM $MgCl_2$ (pH 6.5) (*E. coli* FtsZ assembly buffer); its light scattering was monitored at 30 °C (as described above, except for a 32- or 64-fold more sensitive ordinate scale); and assembly was initiated with 1 mM GTP. FtsZ samples were adsorbed to carbon-coated grids, negatively stained with 2% uranyl acetate, and observed under Jeol 1200 EX electron microscopes.

[2] M. A. Oliva, and J. M. Andreu, unpublished data.

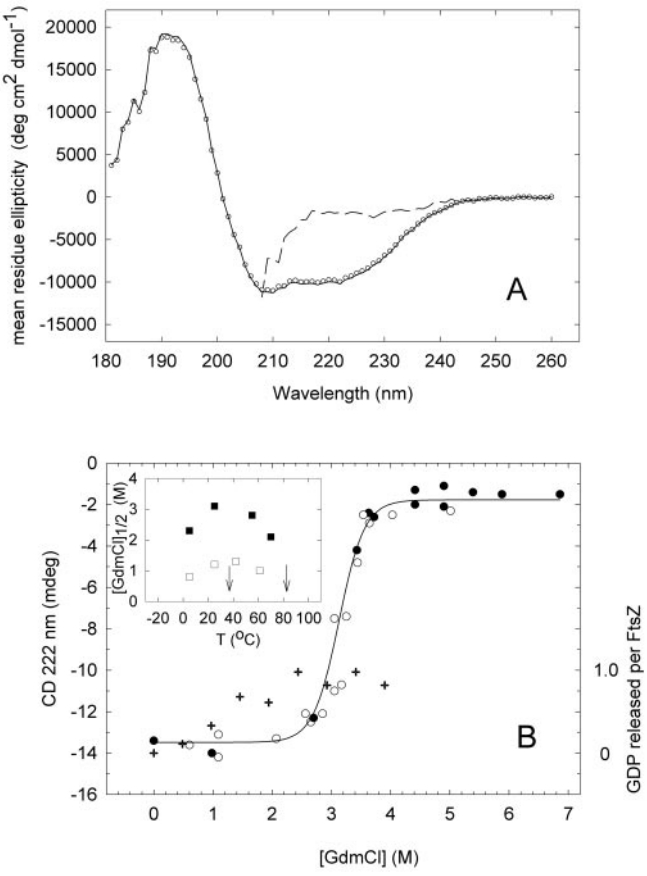

FIG. 1. *A*, CD spectra of *M. jannaschii* FtsZ at 25 °C. *Solid line*, native FtsZ dialyzed against 20 mM Pipes-KOH and 2 mM DTT (pH 7.5); *dashed line*, FtsZ unfolded with 6 M GdmCl in same buffer; *circles*, FtsZ refolded from 6 M GdmCl by dialysis as described under "Experimental Procedures." *B*, equilibrium GdmCl unfolding curve of FtsZ (0.15 mg ml^{-1}) at 25 °C. *Closed circles*, increasing GdmCl concentrations; *open circles*, reverse experiment made by dilution from 5.7 M GdmCl; +, centrifugation measurements of nucleotide released from FtsZ (scale on the *right ordinate*). The *solid line* is a two-state model fit (37) to the collected CD data, yielding $[GdmCl]_{½} = 3.13 \pm 0.04$ M, cooperativity parameter $m = 2740 \pm 340$, and an unfolding free energy change of $\Delta G^0_{app} = 8.6$ kcal mol^{-1} (at 0 M GdmCl). *Inset*: *closed squares*, $[GdmCl]_{½}$ values determined at several temperatures; *open squares*, values for the second transition of the unfolding of *E. coli* FtsZ (see Fig. 3). The *arrows* at 37 and 85 °C mark the optimal growth temperatures of *E. coli* and *M. jannaschii*, respectively.

RESULTS AND DISCUSSION

Equilibrium Unfolding of Archaeal FtsZ—FtsZ from *M. jannaschii* and from *E. coli* and tubulin from calf brain have similar far-ultraviolet CD spectra (Figs. 1*A*, 3*A*, and 4*A*, respectively) characterized by a maximum at 190–192 nm (~20,000 degrees cm^2 dmol^{-1}) and two minima at 209 and 220–222 nm (in the range of −10,000 to −13,000 degrees cm^2 dmol^{-1}), with slightly different shapes (CD_{222}/CD_{209} ratios of 0.91 for *M. jannaschii* FtsZ, 0.83 for *E. coli* FtsZ, and 1.01 for tubulin). The solution conditions employed (without added Mg^{2+}) favor unassociated *E. coli* FtsZ monomers (32) and tubulin $\alpha\beta$-dimers (39); *M. jannaschii* FtsZ shows incipient oligomerization, which can be reduced by ionic strength (28). The three spectra were insensitive to protein concentration (0.1–2 mg ml^{-1}). The similarity of these CD spectra could be expected from the large sequence conservation between archaeal and bacterial FtsZ (37% identical residues) and the extended secondary structural conservation between FtsZ and tubulins despite their low sequence identity (6, 40).

M. jannaschii FtsZ rapidly acquired a CD spectrum characteristic of disordered polypeptides in >5 M GdmCl (Fig. 1*A*, *dashed line*). Remarkably, when the denaturant was dialyzed in the cold, *M. jannaschii* FtsZ recovered a CD spectrum indistinguishable from the native spectrum (Fig. 1*A*, *circles* and *solid line*, respectively). Similar results were obtained with 10 μM GDP, 10 μM GTP, or without nucleotide in the dialysis buffer; these dialyzed samples contained 1.0 mol (GDP), 0.8 (GTP), and 0.5 (no addition) of nucleotide/FtsZ, respectively. Similar CD results were also obtained upon 50-fold dilution of FtsZ solutions in 6 M GdmCl into buffer at 2, 25, or 53 °C (data not shown). At 80 °C, there was a 20% decrease in the CD value at 222 nm without denaturant with respect to the value at 25 °C, suggesting a partial thermal unfolding of the protein. At this high temperature, *M. jannaschii* FtsZ partially refolded upon dilution to an extent of ~45% from a comparison with the CD values of the controls at 222 nm.

Determination of the equilibrium GdmCl unfolding-refolding curve of *M. jannaschii* FtsZ at 25 °C from the CD data at 222 nm indicated a single-stage transition between ~2.2 and 4 M GdmCl, which was fully reversible within experimental error and had a $[GdmCl]_{½}$ (midpoint) at 3.1 M GdmCl (Fig. 1*B*). There is no evidence for any residual structure above 5 M GdmCl. The curve could be fitted by a two-state equilibrium model (Fig. 1*B*, *solid line*), suggesting (but not proving) that both domains of *M. jannaschii* FtsZ unfold simultaneously. Deletion of the unnatural C-terminal Gly-Ser-His_6 extension from the *M. jannaschii* FtsZ protein had no significant effect on the GdmCl unfolding-refolding curve. The $[GdmCl]_{½}$ values determined at three other temperatures from the change in the CD value at 222 nm were as follows: 5 °C, 2.3 M; 55 °C, 2.8 M; and 70 °C, 2.2 M (Fig. 1*B*, *inset*). This indicates that *M. jannaschii* FtsZ is maximally stabilized at ~40 °C, and it is less stable in the cold and at higher temperatures; from the trend of the data, FtsZ may be marginally stable at the 85 °C optimal growth temperature of *M. jannaschii* (41).

Monitoring the unfolding of *M. jannaschii* FtsZ by the change in fluorescence emission intensity of its single tryptophan (Trp^{319}, which is in the second domain, roughly diametrically opposite of the nucleotide-binding site) indicated a similar transition centered at 3.2 M GdmCl (data not shown). However, the release of the nucleotide bound to FtsZ, measured in the solution after sedimenting the protein, took place at lower denaturant concentrations (midpoint of ~1.5 M GdmCl), at which the CD change was practically negligible (nucleotide release was confirmed by chromatography in Sephadex G-25 columns equilibrated in 1 and 2 M GdmCl). This indicates that the average secondary structure of *M. jannaschii* FtsZ at 25 °C is practically insensitive to GDP binding and that the unfolding measured by CD spectroscopy is that of the apoprotein. However, the nucleotide binding must further stabilize the native protein, and it is known to induce local structural changes in *M. jannaschii* FtsZ (28). *M. jannaschii* FtsZ in 6 M GdmCl could be separated from the nucleotide by chromatography on Sephadex G-25 (Fig. 2, *curves a*; 0.9 mol of nucleotide released per FtsZ). However, when unfolded *M. jannaschii* FtsZ was diluted from 6 to 0.12 M GdmCl in the cold and chromatographed on a column without denaturant, the protein bound again ~80% of its released nucleotide (Fig. 2, *curves b*; 0.2 mol of nucleotide released per FtsZ), even in this experiment carried out in the absence of added nucleotide. This indicate that GdmCl-unfolded *M. jannaschii* FtsZ can easily regain functionality.

Equilibrium Unfolding of Bacterial FtsZ—E. coli FtsZ unfolded in GdmCl (Fig. 3*A*, *dashed line*), and it refolded upon dilution of the denaturant in 20 mM Pipes and 5 mM DTT (pH 7.5) at 25 °C, as judged from the CD spectra, in which 93–97% of the 222 nm ellipticity of the native protein was typically recovered (Fig. 3*A*, *open circles* and *solid line*, respectively). A

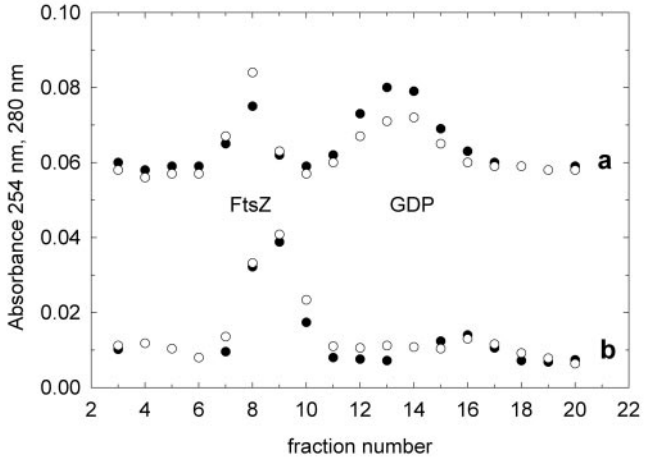

FIG. 2. **Nucleotide binding by refolded *M. jannaschii* FtsZ.** *Curves a*, FtsZ (6.4 nmol) released its bound nucleotide in 6 M GdmCl, as determined by chromatography on a Sephadex G-25 column (0.9 × 25 cm; 1-ml fractions) equilibrated in 6 M GdmCl and 10 mM sodium phosphate (pH 7.0) at 25 °C and by spectrophotometric measurement. *Closed circles*, absorbance measurements at 254 nm; *open circles*, absorbance measurements at 280 nm (there were 5.6 nmol of FtsZ in the first peak and 5.3 nmol of released guanine nucleotide in the second peak). *Curves b*, FtsZ held in 6 M GdmCl (0.4 mM FtsZ, 0.016 ml, 30 min, 25 °C) was diluted 50-fold into cold buffer without denaturant and then chromatographed on a similar Sephadex G-25 column equilibrated in 20 mM Pipes-KOH and 1 mM DTT (pH 7.5) at 5 °C. FtsZ bound again most of its nucleotide (the first peak contained ~6 nmol of FtsZ, and the second peak decreased to 1.1 nmol of released guanine nucleotide).

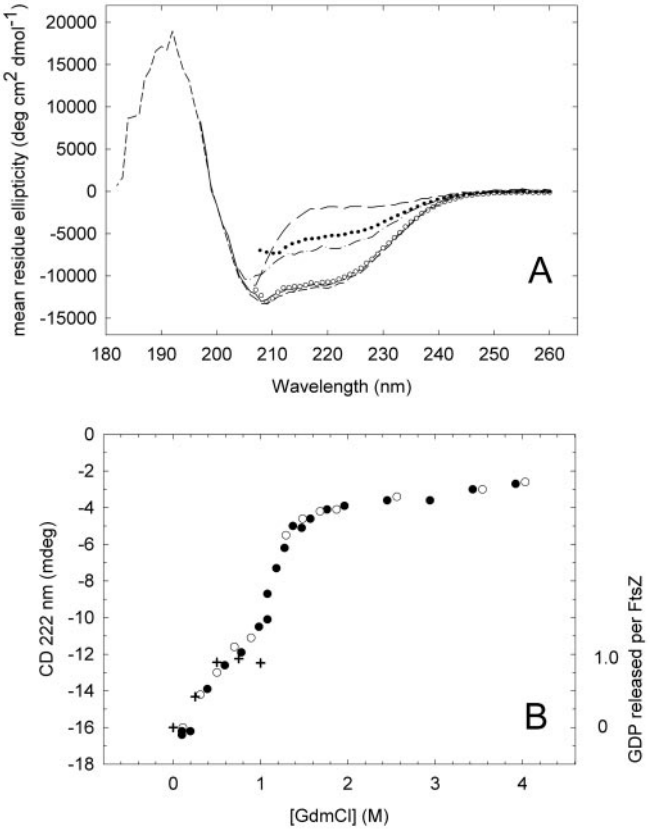

FIG. 3. *A*, CD spectra of *E. coli* FtsZ at 25 °C. *Short-dashed* and *solid lines*, native FtsZ in 20 mM Pipes-KOH and 5 mM DTT (pH 7.5) with 0 M and 0.1 M GdmCl, respectively; *long-dashed line*, unfolded FtsZ in 4 M GdmCl; *open circles*, FtsZ refolded from 5.7 M GdmCl by 50-fold dilution; *dashed-dotted line*, FtsZ in 1 M GdmCl; *closed circles*, FtsZ refolded by dilution from 5.7 to 1.11 M GdmCl. *B*, equilibrium unfolding of FtsZ (0.20 mg ml^{-1} in same buffer at 25 °C) (*circles*) and nucleotide release from FtsZ (+). An unfolding-refolding curve in the buffer employed for the nucleotide release measurements (20 mM Pipes-KOH, 250 mM KCl, 2 mM TCEP, and 10 μM GDP (pH 7.5)) gave similar results.

similar result was obtained in 100 mM potassium glutamate, 200 mM potassium acetate, 5 mM magnesium acetate, and 20 mM Hepes-KOH (pH 7.5) (potassium glutamate-acetate buffer), resembling the physiological osmolytes in the *E. coli* cytoplasm (42) (within the experimental error from subtracting the dichroism of L-glutamate). The spectrum obtained by dilution in ice-cold *E. coli* FtsZ assembly buffer containing 5 mM DTT (pH 6.5) matched the CD spectrum of the native control. However, complete refolding of *E. coli* FtsZ was not obtained by dialysis (in Pipes/DTT or *E. coli* FtsZ assembly buffer/DTT with 10 μM GTP), in which this protein partially refolded and lost most of the nucleotide (data not shown).

E. coli FtsZ was very sensitive to low concentrations of GdmCl. Its 25 °C equilibrium unfolding-refolding curve showed two reversible stages (Fig. 3*B*). The first stage had an amplitude of ~30% of the total change and took place between 0.1 and 0.8 M GdmCl; the second stage proceeded between ~1 and 1.6 M GdmCl (Fig. 3*B*). Monitoring the unfolding of *E. coli* FtsZ with the emission intensity of the tyrosines showed a change centered at ~1 M GdmCl, compatible with the CD results (data not shown). The first CD stage coincided with the release of bound GDP, suggesting that ordering of part of the secondary structure of *E. coli* FtsZ, perhaps at its nucleotide-binding domain, is induced by nucleotide binding. It should be noted that GDP was relatively inefficiently bound by *E. coli* FtsZ at low ionic strength. It was spontaneously released from *E. coli* FtsZ in 20 mM Pipes (pH 7.5) containing 0 or 2 mM TCEP and 10 μM GDP (0.8 mol of GDP released per FtsZ during a 2-h centrifugation at 25 °C). The nucleotide loss was reduced by 50 mM KCl, by 50 mM NaCl, or by 5 mM $MgCl_2$ (0.2–0.3 mol of GDP released per FtsZ) and suppressed by 250 mM KCl or potassium glutamate-acetate buffer (0.0 mol of GDP released per FtsZ). *E. coli* FtsZ chromatographed on Sephadex G-25 columns equilibrated in the same buffer with 250 mM KCl released <0.04 mol of GDP at 25 °C (2 h), but ~0.8 mol of GDP at 42 °C (1.5 h). Dilution-refolded *E. coli* FtsZ was able to bind GTP and to hydrolyze it similarly to the native protein, as indicated by the assembly experiments described below. The $[GdmCl]_{½}$ values of the second unfolding transition were ~0.8 M at 5 °C, 1.2 M at 25 °C, 1.3 M at 42 °C, and 1.0 M at 61 °C. At 42 and 61 °C in the absence of denaturant, the CD value at 222 nm was ~80% of the value at 25 °C, and only a single transition was observed, suggesting that the first transition had been thermally induced and that the observed (second) transition is the unfolding of the apoprotein.

Comparison of the GdmCl unfolding of FtsZ from *E. coli* and from *M. jannaschii* shows important differences. The results suggest that the native structure of *E. coli* FtsZ is stabilized by nucleotide binding. In contrast, no effect of the tightly bound nucleotide on the more stable secondary structure of *M. jannaschii* FtsZ was observed. A thermophilic protein may be stabilized with respect to its mesophilic homologs at 25 °C by an extension or increase of the stability parabola, rather than by a shift to higher temperatures (43). An approximate comparison of the unfolding $[GdmCl]_{½}$ *versus* temperature profiles of FtsZ from *M. jannaschii* and from *E. coli* (Fig. 1*B*, *inset*) shows that (i) the thermophilic apoprotein was much more stable that mesophilic FtsZ over a similar temperature range; and (ii) at the optimal growth temperatures of their respective organisms, the stability of both proteins should be comparably low. In the macromolecularly crowded prokaryotic cytosol, macromolecules that do not bind FtsZ should stabilize its com-

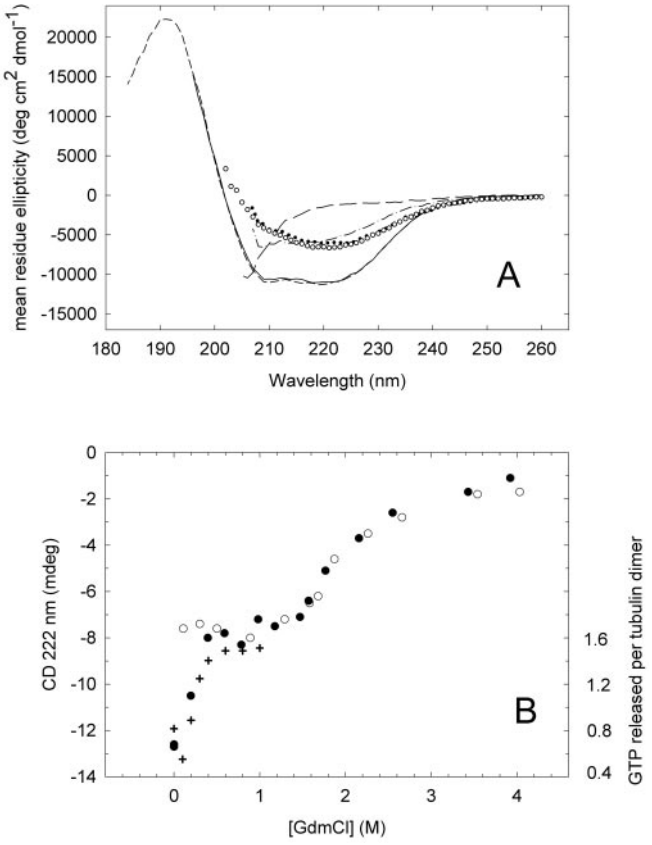

FIG. 4. *A*, CD spectra of tubulin from bovine brain. *Short-dashed* and *solid lines*, native tubulin with 0 and 0.12 M GdmCl, respectively, in 10 mM sodium phosphate and 5 mM DTT (pH 7.0); *long-dashed line*, unfolded tubulin in 4.5 M GdmCl; *open circles*, tubulin misfolded from 5.5 M GdmCl by 50-fold dilution; *dashed-dotted line*, tubulin in 1 M GdmCl; *closed circles*, tubulin misfolded by dilution from 5.5 to 1.12 M GdmCl. *B*, unfolding curve of tubulin (0.15 mg ml^{-1}) (*closed circles*) and the reverse experiment (*open circles*) made by dilution from 5.9 M GdmCl (same buffer at 25 °C). +, measurements of nucleotide released from tubulin (scale on the *right ordinate*).

pact native structure relative to the less compact unfolded forms due to a volume exclusion effect (44), and nonspecific aggregation of FtsZ folding intermediates might be prevented by molecular chaperones (17).

Non-reversible Unfolding of Eukaryotic Tubulin—Similar unfolding-refolding experiments were performed with bovine brain tubulin. Unlike FtsZ, the GdmCl unfolding of tubulin was not reverted upon dilution of the denaturant, but the protein misfolded into a state characterized by a CD spectrum with a single minimum at ~220 nm (Fig. 4*A*, *open circles*) and about half the ellipticity of native tubulin (*short-dashed* and *solid lines*). The shape of this spectrum is suggestive of a β-sheet aggregate formed in the absence of denaturant from the previously unfolded protein. Dilution into cold glycerol-containing assembly buffer (10 mM sodium phosphate, 3.4 M glycerol, 6 mM $MgCl_2$, 1 mM EGTA, and 0.1 mM GTP, pH 6.5) gave a similar misfold. The equilibrium unfolding curve of tubulin monitored by CD spectroscopy at 222 nm showed (like that of *E. coli* FtsZ) two stages; the first one took place below 0.6 M GdmCl and encompassed the dissociation of 1.6 mol of bound GTP/tubulin αβ-dimer (Fig. 4*B*; tubulin underwent a spontaneous partial release of 0.6 mol of GTP/dimer at 0 M GdmCl during the 1.5-h centrifugation). This was followed by a plateau at ~1 M GdmCl and a second broad unfolding process between ~1.5 and 4 M GdmCl (Fig. 4*B*, *closed circles*). Tubulin had a tendency to precipitate in 1 M GdmCl, but not at higher denaturant concentrations. The reversal curve (Fig. 4*B*, *open circles*) followed the second stage of the denaturation curve; but below 1 M GdmCl, it remained at a practically constant value. This might give the wrong impression, that the second stage of denaturation was reversible and that only the first stage did not reverse. However, the CD spectrum of tubulin after dilution from 6 to 1 M GdmCl (Fig. 4*A*, *closed circles*) was superimposable with that of tubulin misfolded by dilution from 6 to 0.12 M GdmCl (*open circles*), and both were different from the CD spectrum of partially unfolded tubulin in 1 M GdmCl (*dashed-dotted line*). Finally, when tubulin in 1 M GdmCl was diluted to 0.1 M GdmCl, it also acquired an identical misfolded CD spectrum. Therefore, we concluded that neither of the GdmCl denaturation stages of tubulin could be reversed under our experimental conditions. The unfolding of tubulin by urea is known to be multistage (45, 46); low concentrations of guanidinium salts enhance, by charge shielding, tubulin polymerization into aberrant microtubules and aggregates (47). The non-reversible thermal denaturation of αβ-tubulin is independent of having GTP or GDP at the exchangeable β-tubulin site (48).

The structural stability of the tubulin αβ-dimer is linked to the binding of a Mg^{2+} ion coordinated with the GTP permanently bound to the α-subunit (7, 29, 48). Purified tubulin in the absence of divalent cations or stabilizing co-solvents is known to age at neutral pH, with relaxation of its CD spectrum (34, 49). Nucleotide binding also contributes to actin stability (50). It has been proposed to participate in the final stage of CCT chaperonin-assisted folding of tubulin (26, 51), which is supported by the observation that the nucleotide release coincided with the first stage of tubulin unfolding (Fig. 4*B*).

Assembly of Refolded FtsZ from M. jannaschii and from E. coli—To confirm the functionality of refolded FtsZ, its assembly was qualitatively characterized. Similar to native *M. jannaschii* FtsZ, FtsZ refolded from 6 M GdmCl by dialysis underwent GTP- and Mg^{2+}-dependent assembly, as monitored by light scattering (Fig. 5*A*, *traces a* and *b*, respectively). *M. jannaschii* FtsZ consumed GTP (Fig. 5*A*, *trace c*), and both the native and refolded proteins reversibly formed cable-like filamentous polymers (Fig. 6*A*), the assembly mechanism of which will be described in detail elsewhere.[2] From these results, we concluded that spontaneously refolded *M. jannaschii* FtsZ assembles similarly to the native protein.

E. coli FtsZ dialyzed in the same buffer as *M. jannaschii* FtsZ or against *E. coli* FtsZ assembly buffer partially recovered its assembly ability (~40–50% of the GTP-specific light scattering), but it formed curly polymers distinct from those of native FtsZ (data not shown). *E. coli* FtsZ refolded by direct 50- and 100-fold dilutions from 6 M GdmCl into *E. coli* FtsZ assembly buffer assembled in a GTP- and Mg^{2+}-dependent manner (Fig. 5*B*, *traces a* and *b*), yielding 50–60% of the maximal light scattering value of the control (*trace c*). Residual GdmCl strongly affected the assembly (Fig. 5*B*, *traces c–e*). Dilution-refolded FtsZ formed thin polymers made of one to several protofilaments (Fig. 6*B*), which were indistinguishable from native protein polymers and are characteristic of *E. coli* FtsZ (32, 52). From these experiments, we concluded that spontaneously refolded *E. coli* FtsZ is able to specifically undergo GTP-dependent self-assembly in a manner qualitatively similar to that of the native protein. Tubulin misfolded from GdmCl formed non-microtubule aggregates (data not shown). Note that purified FtsZ forms inhomogeneous filamentous FtsZ polymers, but that bacterially expressed vertebrate α- and β-tubulin polypeptide chains, once refolded with chaperonin and cofactors, can assemble into microtubules (21).

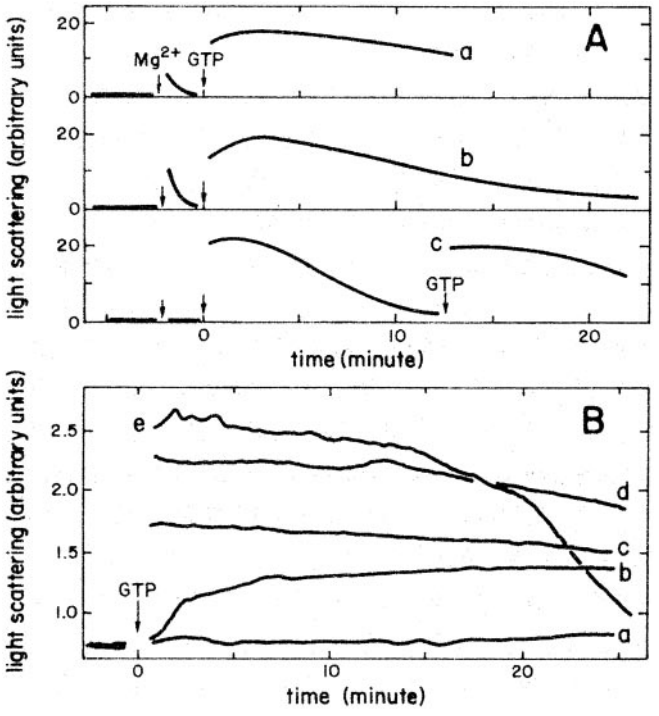

FIG. 5. **Assembly of native and refolded FtsZ monitored by light scattering.** *A*: *trace a*, native *M. jannaschii* FtsZ dialyzed as described in the legend to Fig. 1 and supplemented with *M. jannaschii* FtsZ assembly buffer with 10 μM GTP (12 μM FtsZ); *trace b*, a parallel sample of FtsZ refolded from 6 M GdmCl by dialysis; *trace c*, a control of native FtsZ directly diluted into assembly buffer without GTP (14 μM FtsZ). Assembly at 55 °C was initiated by addition of 6 mM $MgCl_2$ and 1 mM GTP at the points indicated by the *arrows*. *B*: *trace a*, 8 μM *E. coli* FtsZ refolded by dilution from 6 to 0.12 M GdmCl in *E. coli* FtsZ assembly buffer to which 1 mM GDP was added at 30 °C at time 0; *trace b*, same as *trace a*, but with assembly started by 1 mM GTP addition; *traces c–e*, assembly of 8 μM FtsZ in same buffer with 0.12, 0.06, and 0 M GdmCl, respectively.

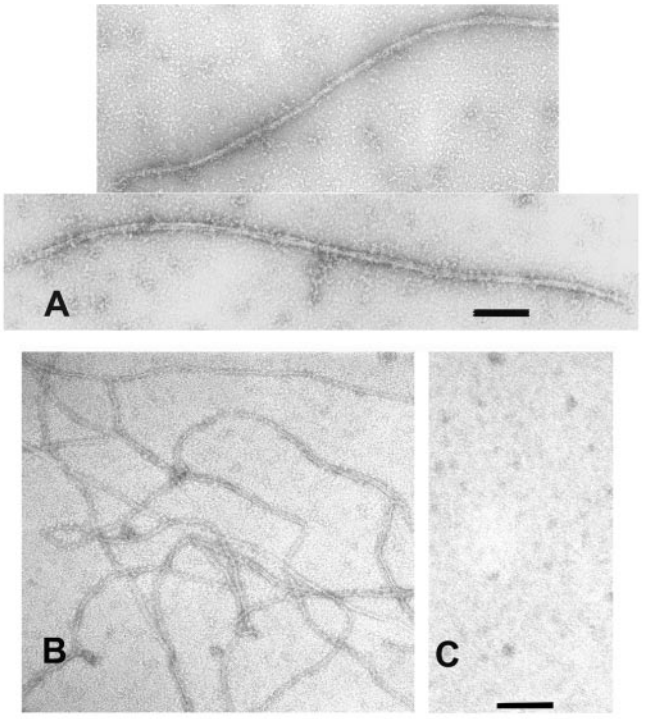

FIG. 6. *A*, electron micrograph of the polymers formed by refolded *M. jannaschii* FtsZ (4 min after GTP addition) (see Fig. 5*A*, *trace b*). *Bar* = 200 nm. *B*, assembly products of dilution-refolded *E. coli* FtsZ (4 μM FtsZ and 0.06 M GdmCl) with 1 mM GTP. *C*, a control with 1 mM GDP. *Bar* = 100 nm.

Analysis of the Tubulin Loop Insertions in the FtsZ/Tubulin Common Core and the Structural Elements Forming Axial and Lateral Contacts in Model Microtubules and Those Binding to CCT—In view of the spontaneous folding of purified FtsZ and the proposal that eukaryotic chaperonin evolved with the actin and tubulin cytoskeleton (25, 26), we asked which tubulin zones require CCT-assisted folding and whether they have a defined role in microtubule assembly. The C-α atoms in the secondary structural elements of the common cores of β-tubulin and FtsZ are superimposable with a 2.4-Å root mean square deviation, which increases to a 4.3-Å root mean square deviation if the loops are included (6). The structure-based sequence alignments of tubulin and FtsZ (Fig. 2 in Ref. 6 and Fig. 3 in Ref. 26) show 10 insertions in α- and β-tubulin monomers with respect to FtsZ (not counting the N- and C-terminal non-homologous portions of both proteins). These insertions locate to tubulin loops and add up to 85–90 extra residues (~30%) over the 300-residue homologous core of FtsZ. However, there are only three small insertions and 9–10 extra residues in FtsZ that are not present in tubulin. The characteristic C-terminal domain of tubulin (helices H11 and H12 and the acidic C termini) replaces S11 and S12 and the C-terminal extensions of FtsZ. Bacterially expressed constructs encompassing the 48 and 52 C-terminal residues of α- and β-tubulin are soluble and can be induced to form H12 with trifluoroethanol (54), suggesting that at least part of the C-terminal domains of tubulin may fold by themselves. On the other hand, complete α- and β-chains from vertebrate tubulin and constructs including their nucleotide-binding or middle domains are typically insoluble,[3] which suggests that these domains of tubulin are unable to fold spontaneously, in contrast with the spontaneous folding of FtsZ. Therefore, it appears that the extensive loop insertions of tubulin contribute to its inability to spontaneously fold. It has not actually been proven whether the main elements responsible are the loop insertions or other features of the same domains such as the solvent-buried interface with the C-terminal domain.

The tubulin loop insertions on the common FtsZ/tubulin fold speak of acquired functional interactions. Inspection of the locations of these insertions (Fig. 7) indicates that they are excluded from the nucleotide-binding sites at the central parts of the axial contact interfaces between tubulin monomers, which are conserved in the FtsZ/tubulin family of protofilament-forming GTPases (8, 15). Instead, they map to more peripheral positions (Fig. 7*A*), at the sides (Fig. 7*B*) and at the back (Fig. 7*C*) of the tubulin monomer. Table I lists the sets of tubulin secondary structural elements that contain insertions (Insert column, 10 elements), those proposed to participate in the axial contacts (Axial column, 11 elements) or in the lateral contacts (Lateral column, eight elements) in model microtubules, and those involved in the tubulin-CCT model contacts (CCT column, eight elements). Inspection of Table I shows that (i) the Insert set does not include the Axial set or vice versa; (ii) the Insert set includes the Lateral set; and (iii) the Insert set includes the CCT set as well, with the exception of the conserved nucleotide-binding loop T7 (26), and the Lateral + CCT sets include the Insert set, except for T7. Regarding the lateral contacts, all the structural elements that have been tentatively associated with the lateral interactions between microtubule protofilaments coincide with one of the loop insertions in the FtsZ/tubulin common core. These elements include the three main zones of lateral contact, which are the M-loop (for micro-

[3] G. Pucciarelli and J. M. Andreu, unpublished data.

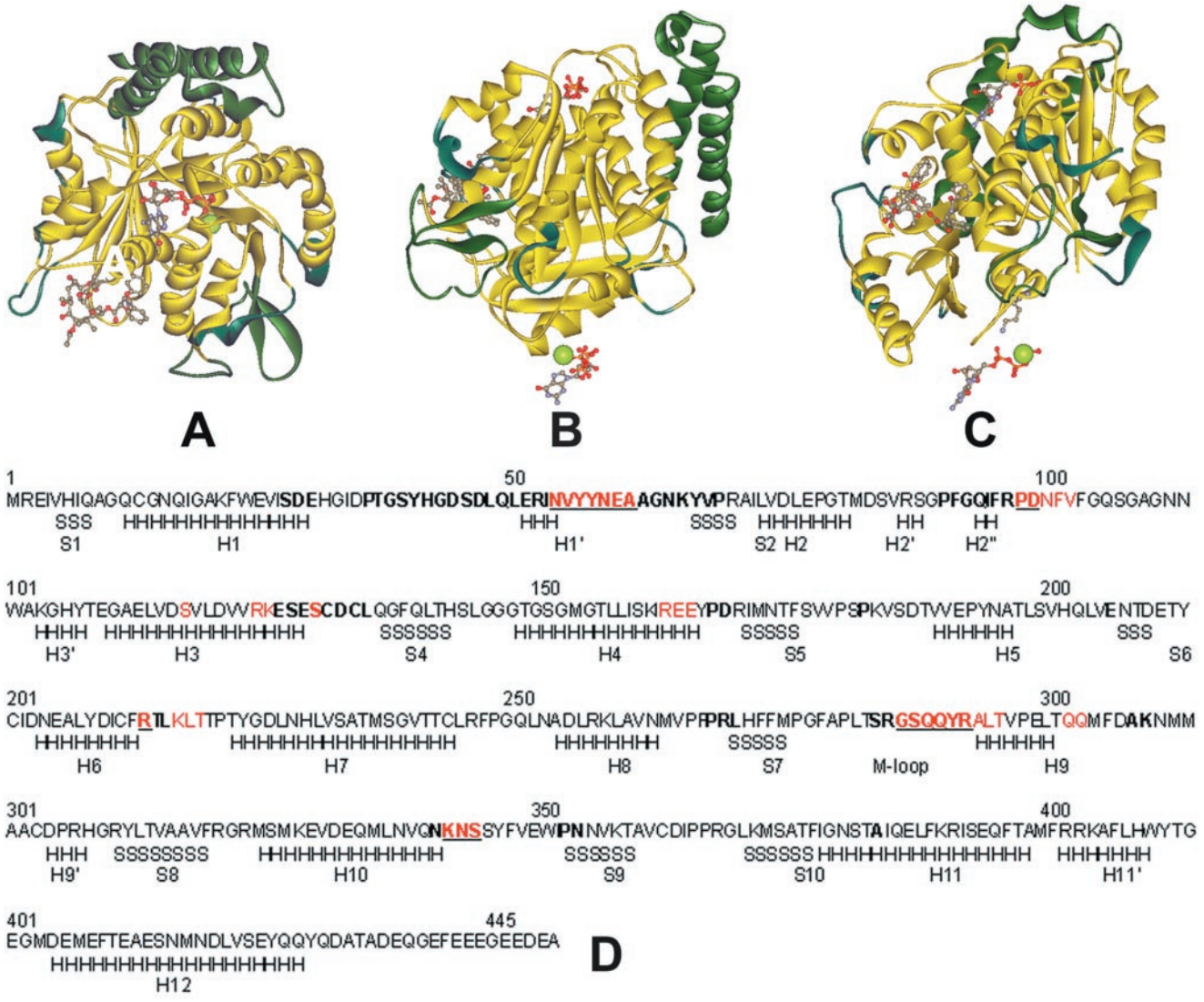

FIG. 7. **Mapping of tubulin zones that are not present in its homolog FtsZ.** *A–C* are ribbon diagrams of β-tubulin (from the αβ-dimer (Protein Data Bank code 1JFF); in *yellow*) in which the residues that are not present in FtsZ (Protein Data Bank code 1FSZ) have been colored *green*. These are the insertions in the FtsZ/tubulin common core and the C-terminal two-helix domain of tubulin. *A*, view from the (+)-end of a protofilament, with the microtubule outside at the top (the GDP bound in the center of the axial interface and Taxol at the luminal face are shown); *B*, tangential view from the side, with the outside at the right (the GTP and Mg^{2+} bound to the α-tubulin subunit of the dimer are shown at the bottom); *C*, view from the inside of a microtubule. *D* shows the sequence of pig brain β-tubulin, in which the tubulin insertions in a structure-based alignment of tubulins and FtsZ (Fig. 3 in Ref. 26) are marked in *boldface*, the residues within lateral contact distance in model microtubules (Fig. 5 in Ref. 9) are in *red*, and residues both in insertions and in lateral contact are *underlined* and in *boldface red*. The secondary structural elements (7) are marked *H* (helix) and *S* (sheet) or are unmarked (loop). Note that from 37 residues of β-tubulin involved in lateral contacts in model microtubules, 24 are at the insertion loops, 12 flank insertion loops, and 1 is in the middle of helix H3.

tubule loop), H3 and its C-terminal loop, and part of the long H1–S2 loop (6, 10). Moreover, even at the residue level, all but one of the residues listed within lateral contact distance in model microtubules (9) are associated with insertion loops (Fig. 7*D*). Based on this analysis, we propose that the loop insertions of tubulin coevolved with the lateral protofilament association to form microtubules, an ability that has not been observed at all in its protofilament-forming homolog FtsZ. As an interesting analogy, subunit/subunit interactions within actin filaments (a twisted pair of protofilaments) involve sequence insertions that are not present in the bacterial homolog MreB and that can make different contacts in F-actin polymorphs (55); in contrast to actin, filamentous MreB consists of pairs of straight parallel protofilaments (1).

It has been suggested that CCT coevolved with tubulin to counteract the folding problems associated with new zones involved in polymerization (26). With regard to the eight zones of tubulin that are in contact with the chaperonin in tubulin-CCT model complexes (Table I, CCT column), five are involved in lateral interactions in microtubules, two correspond to the tubulin insertion loops that are not involved in lateral interactions (loops H8–S7 and S9–S10), and the other is conserved loop T7. This is a remarkable correlation, considering that CCT encircles open tubulin monomers, entailing a binding topology different from that of tubulin dimers in the microtubule wall. Accepting that the present tubulins and FtsZ arose from a common protofilament-forming ancestor, we suggest that the CCT-assisted folding of tubulin specifically coevolved with the lateral association interfaces responsible for extended two-dimensional polymerization into microtubules. The coevolution of the tubulin loop inserts with the lateral microtubule contacts and hence CCT-assisted folding is supported by the different nature of the lateral contacts in FtsZ polymers and microtubules, which is outlined below.

TABLE I

Structural elements of the FtsZ/tubulin common core that have insertions in tubulin (Insert column, insertions larger than a single residue), that have been proposed to take part in axial interactions (Axial column) or in lateral interactions (Lateral column) between tubulin molecules in microtubules, or that bind to chaperonin (CCT column)

Structural element[a]	Insert[a,b]	Axial[c]	Lateral[c,d]	CCT[b]
T1 (S1–H1) loop		X		
H1–S2 loop	X		X	X
T2 (S2–H2) loop		X		
H2–S3 loop	X		X	X
T3 (S3–H3) loop		X		
H3/H3–S4 loop	X	X	X	X
H4/H4–S5 loop	X		X	X
T5 (S5–H5) loop		X		
H6–H7 loop	X	X	X	
T7 (H7–H8) loop		X		X
H8/H8–S7 loop	X	X		X
M (S7–H9) loop	X		X	X
H9/H9–S8 loop	X		X	
H10		X		
H10–S9 loop	X	X	X	
S9/S9–S10 loop	X[e]	X		X

[a] Ref. 6.
[b] Ref. 26. CCT binding zones include the tubulin H11–H12 loop as well.
[c] Ref. 8. Axial contact zones include the tubulin H11–H12 loop as well.
[d] Ref. 9.
[e] This insertion is present only in α-tubulins.

Comparison of Tubulin with FtsZ Assemblies Suggests That the Elemental Polymer Formed by Purified FtsZ Is a Distinct Double-stranded Filament with a Non-propagated Lateral Contact—Microtubules are pseudo-helical polymers formed by parallel protofilaments of $\alpha\beta$-tubulin dimers; the tubulin dimers laterally associate by propagated homologous α/α and β/β lateral interactions (it is only microtubule cylindrical closure that involves related α/β and β/α interactions) (for review, see Ref. 56). The less well defined assembly products of FtsZ monomers *in vitro* are made of tubulin-like protofilaments (14, 15) that associate in diverse manners (Fig. 6). Although purified *M. jannaschii* FtsZ can form, with Ca^{2+} and GMPCPP, cable-like helical tubes of lengths comparable to the inner circumference of a bacterium (57), the assembly of FtsZ proteins typically yields a variety of filamentous polymers and sheets. Assembly of *M. jannaschii* FtsZ is cooperative.[4] A basic pattern in the assembly of *M. jannaschii* FtsZ is the lateral association of two FtsZ parallel protofilaments with an axis of symmetry between them, forming thick filaments; the thick filaments associate into larger polymers such as cables and sheets of antiparallel thick filaments (15),[2] using lateral interactions necessarily different from those forming the protofilament pair. The protofilament pairing interface of FtsZ in the model thick filament (15) approximately corresponds to the microtubule luminal face of tubulin. This association pattern is clearly incompatible with the formation of microtubule-like two-dimensional polymers in which the same lateral interactions that form a protofilament pair propagate across the polymer width. Purified bacterial FtsZ typically assembles into polymers made of few protofilaments (Fig. 6), unless additives such as DEAE-dextran or a lipid surface is employed (14, 32, 52, 53, 58, 59). *E. coli* FtsZ forms *in vivo* highly dynamic assemblies (60), the nature of which remains elusive; it is possible that they also have a limited two-dimensionality, consisting of very few protofilaments stabilized by interaction with other septal proteins.

Conclusions—In this work, we have analyzed the folding and assembly of archaeal and bacterial FtsZ in comparison with the eukaryotic structural homolog tubulin. The GdmCl-induced unfolding of FtsZ proteins from *M. jannaschii* and *E. coli* was essentially reversible, unlike that of tubulin. Both FtsZ and tubulin released their bound nucleotide at relatively low GdmCl concentrations. In the case of *E. coli* FtsZ and tubulin, this coincided with the first unfolding stage of both proteins at 25 °C, which was followed by other unfolding process(es), suggesting a nucleotide-dependent structural stabilization. However, dissociation of the nucleotide tightly bound to *M. jannaschii* FtsZ insignificantly modified the secondary structure of this protein, which unfolded in a single stage at higher GdmCl concentrations. Isolated FtsZ polypeptide chains were capable of spontaneous folding, followed by GTP-dependent self-assembly. It is not known whether FtsZ folding may be further facilitated by molecular chaperones, but its assembly is modulated by other cell division proteins. On the other hand, tubulin did not fold spontaneously, but did fold with the assistance of the eukaryotic chaperonin CCT. Analysis of the extensive tubulin insertion loops in the FtsZ/tubulin common core and of the contacts in model microtubules and tubulin-CCT complexes suggests that the loop insertions of tubulin and its CCT-assisted folding coevolved with the lateral association interfaces responsible for extended two-dimensional polymerization into microtubules. This proposal is supported by comparison of microtubules with the distinct paired protofilament FtsZ polymers.

Acknowledgments—We thank Drs. J. F. Díaz, S. Huecas, M. Menendez, G. Rivas, M. Vicente, and J. M. Valpuesta (Consejo Superior de Investigaciones Científicas, Madrid) for helpful discussions and Maribel López (Departamento de Biología, Universidad de Chile) for technical help.

[4] S. Huecas and J. M. Andreu, unpublished data.

REFERENCES

1. van den Ent, F., Amos, L. A, and Löwe, J. (2001) *Nature* **413,** 39–44
2. Löwe, J., and Amos, L. A. (1998) *Nature* **391,** 203–206
3. Jones, L. J. F., Carballido-Lopez, R., and Errington, J. (2001) *Cell* **104,** 913–922
4. Rothfield, L., Justice, S., and Garcia-Lara, J. (1999) *Annu. Rev. Genet.* **33,** 423–448
5. Nogales, E., Wolf, S. G., and Downing, K. H. (1998) *Nature* **391,** 199–203
6. Nogales, E., Downing, K. H., Amos, L. A., and Löwe, J. (1998) *Nat. Struct. Biol.* **5,** 451–458
7. Löwe, J., Li, H., Downing, K. H., and Nogales, E. (2001) *J. Mol. Biol.* **313,** 1045–1057
8. Nogales, E., Whittaker, M., Milligan, R. A., and Downing, K. H. (1999) *Cell* **96,** 79–88
9. Meurer-Grob, P., Kasparian, J., and Wade, R. (2001) *Biochemistry* **40,** 8000–8008
10. Chacón, P., and Wriggers, W. (2002) *J. Mol. Biol.* **317,** 375–384
11. Bi, E., and Lutkenhaus, J. (1991) *Nature* **354,** 161–164
12. Ben-Yehuda, S., and Losick, R. (2002) *Cell* **109,** 257–266
13. Pichoff, S., and Lutkenhaus, J. (2002) *EMBO J.* **21,** 685–693
14. Erickson, H. P., Taylor, D. W., Taylor, A. K., and Bramhill, D. (1996) *Proc.*

Natl. Acad. Sci. U. S. A. **93,** 519–523
15. Löwe, J., and Amos, L. A. (1999) *EMBO J.* **18,** 2364–2371
16. Yu, X. C., Margolin, W., Gonzalez-Garay, M. L., and Cabral, F. (1999) *J. Cell Sci.* **112,** 2301–2311
17. Hartl, F. U., and Hayer-Hartl, M. (2002) *Science* **295,** 1852–1858
18. Gao, Y., Thomas, J. O., Chow, R. L., Lee, G. H., and Cowan, N. J. (1992) *Cell* **69,** 1043–1050
19. Yaffe, M. B., Farr, G. W., Miklos, D., Horwich, A. L., Sterlicht, M. L., and Sternlicht, H. (1992) *Nature* **358,** 245–248
20. Thulasiraman, V., Yang, C. F., and Frydman, J. (1999) *EMBO J.* **18,** 85–95
21. Shah, C., Xu, C. Z., Vickers, J., and Williams, R. (2001) *Biochemistry* **40,** 4844–4852
22. Houry, W. A., Frishman, D., Eckerskorn, C., Lottspeich, F., and Hartl, U. (1999) *Nature* **402,** 147–154
23. Dobrzynski, J. K., Sternlicht, M. L., Peng, I., Farr, G. W., and Sternlicht, H. (2000) *Biochemistry* **39,** 3988–4003
24. Uehara, T., Matsuzawa, H., and Nishimura, A. (2001) *Genes Cells* **6,** 803–814
25. Llorca, O., Martin-Benito, J., Ritco-Vonsovici, M., Grantham, J., Hynes, G. M., Willison, K., Carrascosa, J., and Valpuesta, J. M. (2000) *EMBO J.* **19,** 6971–6979
26. Llorca, O., Martin-Benito, J., Gomez-Puertas, P., Ritco-Vonsovici, M., Willison, K., Carrascosa, J., and Valpuesta, J. M. (2001) *J. Struct. Biol.* **135,** 205–218
27. Llorca, O., Martin-Benito, J., Grantham, J., Ritco-Vonsovici, M., Willison, K., Carrascosa, J., and Valpuesta, J. M. (2001) *EMBO J.* **20,** 4065–4075
28. Diaz, J. F., Kralicek, A., Mingorance, J., Palacios, J. M., Vicente, M., and Andreu, J. M. (2001) *J. Biol. Chem.* **276,** 17307–17315
29. Correia, J. J., Baty, L. T., and Williams, R. C. (1987) *J. Biol. Chem.* **262,** 17278–17284
30. Edelhoch, H. (1967) *Biochemistry* **6,** 1948–1954
31. Fasman, G. D. (ed) (1992) *Practical Handbook of Biochemistry and Molecular Biology*, pp. 81–83, CRC Press Inc., Boca Raton, FL
32. Rivas, G., Lopez, A., Mingorance, J., Ferrandiz, M. J., Zorrilla, S., Minton, A. P., Vicente, M., and Andreu, J. M. (2000) *J. Biol. Chem.* **275,** 11740–11749
33. Lee, J. C., Frigon, R. P., and Timasheff, S. N. (1973) *J. Biol. Chem.* **248,** 7253–7262
34. Andreu, J. M., and Timasheff, S. N. (1982) *Biochemistry* **21,** 6465–6476
35. Andreu, J. M., Perez-Ramirez, B., Gorbunoff, M. J., Ayala, D., and Timasheff, S. N. (1998) *Biochemistry* **37,** 8356–8368
36. Ludueña, R. F. (1998) *Int. Rev. Cytol.* **178,** 207–275
37. Pace, C. N., and Scholtz, J. M. (1997) in *Protein Structure, a Practical Approach* (Creighton, T. E., ed) 2nd Ed., pp. 299–321, Oxford University Press, Oxford
38. Eftink, M. (1995) *Methods Enzymol.* **259,** 487–512
39. Frigon, R. P., and Timasheff, S. N. (1975) *Biochemistry* **14,** 4559–4566
40. de Pereda, J. M., Leynadier, D., Evangelio, J., Chacon, P., and Andreu, J. M. (1996) *Biochemistry* **35,** 14203–14215
41. Jones, W. J., Leigh, J. A., Mayer, F., Woese, C. R., and Wolfe, R. S. (1983) *Arch. Microbiol.* **136,** 254–261
42. Record, M. T., Jr., Courtenay, E. S., Cayley, S., and Guttman, H. J. (1998) *Trends Biochem. Sci.* **23,** 190–194
43. Jaenicke, R., and Böhm, G. (1998) *Curr. Opin. Struct. Biol.* **8,** 738–748
44. Minton, A. P. (2000) *Biophys. J.* **78,** 101–109
45. Sackett, D. L., Bhattacharyy, B., and Wolff, J. (1994) *Biochemistry* **33,** 12868–12878
46. Guha, S., and Bhattacharyya, B. (1997) *Biochemistry* **36,** 13208–13213
47. Wolff, J., Knipling, L., and Sackett, D. L. (1996) *Biochemistry* **35,** 5910–5920
48. Menendez, M., Rivas, G., Diaz, J. F., and Andreu, J. M. (1998) *J. Biol. Chem.* **273,** 167–176
49. Prakash, V., and Timasheff, S. N. (1982) *J. Mol. Biol.* **160,** 499–515
50. Schuler, H., Lindberg, U., Schutt, C. E., and Karlsson, R. (2000) *Eur. J. Biochem.* **267,** 476–486
51. Farr, G. W., Scharl, E. C., Schumacher, R. J., Sondek, S., and Horwich, A. L. (1997) *Cell* **89,** 927–937
52. Mukerjee, A., and Lutkenhaus, J. (1999) *J. Bacteriol.* **181,** 823–832
53. Lu, C., Stricker, J., and Erickson, H. P. (1998) *Cell Motil. Cytoskeleton* **40,** 71–86
54. Jimenez, M. A., Evangelio, J. A., Aranda, C., Lopez-Brauet, A., Andreu, D., Rico, M., Lagos, R., Andreu, J. M., and Monasterio, O. (1999) *Protein Sci.* **8,** 788–799
55. Galkin, V., VanLoock, M. S., Orlova, A., and Egelman, E. H. (2002) *Curr. Biol.* **12,** 570–575
56. Nogales, E. (2000) *Annu. Rev. Biochem.* **69,** 277–302
57. Löwe, J., and Amos, L. A. (2000) *Biol. Chem. Hoppe-Seyler* **381,** 993–999
58. Lu, C., Reedy, M., and Erickson, H. P. (2000) *J. Bacteriol.* **182,** 164–170
59. Romberg, L., Simon, M., and Erickson, H. P. (2001) *J. Biol. Chem.* **276,** 11743–11753
60. Stricker, J., Maddox, P., Salmon, E. D., and Erickson, H. P. (2002) *Proc. Natl. Acad. Sci. U. S. A.* **99,** 3171–3175